

Initial data for superposed rotating black holes

William Krivan

*Department of Physics, University of Utah, Salt Lake City, UT 84112
and Institut für Astronomie und Astrophysik, Universität Tübingen, D-72076 Tübingen, Germany*

Richard H. Price

Department of Physics, University of Utah, Salt Lake City, UT 84112

The standard approach to initial data for both analytic and numerical computations of black hole collisions has been to use conformally-flat initial geometry. Among other advantages, this choice allows the simple superposition of holes with arbitrary mass, location and spin. The conformally flat restriction, however, is inappropriate to the study of Kerr holes, for which the standard constant-time slice is not conformally flat. Here we point out that for axisymmetric arrangements of rotating holes, a nonconformally flat form of the 3-geometry can be chosen which allows fairly simple superposition of Kerr holes with arbitrary mass and spin. We present initial data solutions representing locally Kerr holes at large separation, and representing rotating holes close enough so that outside a common horizon the spacetime geometry is a perturbation of a single Kerr hole.

04.25.Dm, 95.30.Sf, 97.60.Lf

I. INTRODUCTION AND OVERVIEW

The study of black hole collisions has been of recent interest in connection with the development of gravitational wave detectors [1], and as a proving ground for numerical relativity [2]. In addition, it will give unprecedented insights into the nonlinear workings of relativistic gravitation in strong field situations.

The approach in numerical work has usually been to use the prescription of Bowen and York [3] to generate initial data representing the holes. In this prescription, the initial value problem is greatly simplified by the assumption that the initial geometry is conformally flat. This approach, though, has some disadvantages for studying collisions with net angular momentum, since the final hole formed will be a Kerr hole, and — at least for standard slicings — the spatial geometry of a Kerr hole is not conformally flat. This means that computations of radiation from coalescence will contain early radiation due to the relaxation of Bowen-York holes to Kerr holes, as well as radiation more directly attributable to the coalescence itself. Still, this represents an astrophysical imperfection rather than a major obstacle to numerical work. For analytic work, however, it is useful to consider initial configurations close to the final stationary hole so that the initial configuration, and the evolution, can be treated with perturbation theory [4]. This technique is inherent in the methods used for extraction of radiation [5] in full numerical relativity. First and second-order perturbation theory have also been remarkably successful in the “close limit approximation,” the analysis of collisions starting from small separations [6–15].

In this paper we present an approach to the generation of initial data that fits the needs of perturbative analysis. Since this approach has essentially the same computational simplicity as that in the conformally flat approach, it is our hope that these solutions will be considered as starting points for numerical relativity evolution. In recent work, comparisons [7,13] between analytic and numerical results have been very helpful to both efforts.

Within the context of a more general formalism, we will present two families of initial data solutions. The first family of solutions will represent an axisymmetric superposition of two equal mass Kerr holes, parameterized by the mass of each hole and the spin of each hole, and a measure of the separation between them. The solution will have the crucial feature that the holes have local “Kerricity.” That is, in a region around each hole small compared to the spacing between the holes, the 3-geometry and extrinsic curvature will have the form of the Kerr initial data, aside from corrections that vanish in the limit of infinite separation. The specific solution given serves to illustrate a method of superposition which can be generalized in an obvious way to a large number of axisymmetric initial configurations. In particular, it can be used to construct initial data for unequal (different mass, different spin) Kerr holes, for more than two holes, for a collection of Kerr and Bowen-York spinning holes, or for a collection of Bowen-York holes (although in this last case the method involves only conformally flat geometries and is equivalent to the Bowen-York method). For any solution constructed by this method the hole will locally have the same form as if it were isolated.

A very important feature of these solutions is their close limit. If we reduce the separation between two holes, an initial horizon will surround both holes, but in the limit of small separation the solution outside that horizon is not a single Kerr hole. This is very different from what happens for nonrotating holes, and this difference is one of the major points we wish to make in this paper. The fact that the Kerr geometry is not the “natural” close limit for a

sequence of initial data sets for two locally Kerr holes is not a flaw in our superposition method, but is to be expected for general initial data sets.

The fact that the close limit of rotating holes is not a Kerr hole is surprising because it is so very different from the Schwarzschild case. For initial value solutions for two nonspinning holes, such as the solutions of Misner [16] or of Brill-Lindquist [17], if the separation between the holes is reduced one expects an all-encompassing horizon to exist on the initial hypersurface, and for the initial value solution outside that initial horizon to approach the Schwarzschild geometry. And this is just what happens [6,18]. In the mathematics, as in intuition, the only source of nonsphericity is the separation of the initial holes, and as that separation is reduced, the solution outside the event horizon becomes spherical, and hence becomes Schwarzschild initial data.

Crucial to the simplicity of this process is the fact that the Schwarzschild initial data is singled out by the requirement of sphericity. The Kerr initial solution, by contrast, requires much more: a set of relationships involving the initial extrinsic curvature as well as the initial 3-geometry. If these relationships are satisfied for the individual holes, there is no reason for them to be satisfied by the superposition of two holes. One can see a rough quantitative sign of this in the following. For a rotating hole of mass M and angular momentum J , the quadrupole moment in the 3-geometry has a magnitude of order J^2/M . If we add two such holes we expect to infer from the distant geometry that we have approximately twice the mass, twice the angular momentum, and (from the $1/r^2$ part of g_{00}) twice the quadrupole moment. The quadrupole moment will therefore be too small by a factor of two for the result to be a Kerr hole. In a manner of speaking, then, what makes two Kerr holes different from a single hole is not simply the separation, it is the more basic fact that there are two of them. There is a completely different point of view from which this can be understood. The Kerr solution is singled out as a spacetime geometry with a stationary horizon. The initial value solution — the 3-geometry and extrinsic curvature — are not special as initial value solutions. By contrast, the initial value solutions for Schwarzschild (spherical 3-geometry, zero extrinsic curvature) is special.

We are pointing out here that the Kerr close limit should not be expected from the superposition of two Kerr holes. This should not be confused with the fact that the Kerr geometry is the natural late time result for the *evolution* of two holes. Due to the evolution, the geometry and extrinsic curvature on a late hypersurface, outside the final horizon, will have approximately Kerr form. For that reason, it is useful to have solutions available with a Kerr close limit.

In Sec. III below we construct such a solution. This solution is somewhat contrived, but any other multihole solution with a Kerr close limit will also be contrived (except of course, the solution produced by evolution). Our particular contrived solution has the unappealing feature that there is a singularity where there should not be a physical reason for a singularity. Since this contrived solution is meant to be used only for small separations, in which case this singularity will be well inside the horizon surrounding the two initial holes. In judging the importance of this singularity, it is necessary to keep in mind the use to which the close-limit solution is to be applied. For this initial value solution (or any other initial value solution with a Kerr close limit) it is possible to use close-limit perturbation theory to find the outgoing radiation generated in the evolution of the initial data. If these initial data are used for numerical relativity, very useful comparisons with analytic results are possible. For such comparisons the unwanted singularity is of concern only if it causes problems in the numerical method. For numerical relativity computations that use horizon excision the singularity should be of no concern whatever.

An alternative approach has recently been given by Baker and Puzio [19] to the construction of initial data sets for axially symmetric non-conformally flat, initial data. That method starts with a specification of the 3-geometry and solves for partial information about the extrinsic curvature. The method has the advantage, in principle, of allowing generalization to a broader class of axisymmetric solutions, in particular to rotating holes which are initially moving. The method has the disadvantage that it is more difficult to implement, and has not yet been tested numerically.

The remainder of the paper is organized as follows: In Sec. II we present the basic method of superposition, and the numerical solution for two identical “locally Kerr” holes, including a numerical demonstration of local Kerricity. In Sec. III we show that the locally Kerr solutions of Sec. II do not have a Kerr close limit, and we introduce solutions that do have a Kerr close limit. A discussion and conclusions are presented in Sec. IV.

II. MATHEMATICAL APPROACH

We start with the Brill-wave [20] form of the metric, as studied by Brandt and Seidel [21–23]. In place of their radial coordinate η which is appropriate to the description of both sides of a throat, we use the alternative coordinate \bar{r} , related to η by $d\eta = d\bar{r}/\bar{r}$. In terms of this coordinate, and the Brandt-Seidel notation, the form of the metric is

$$ds^2 = \Phi^4 \left[e^{-2q} (d\bar{r}^2 + \bar{r}^2 d\theta^2) + \bar{r}^2 \sin^2 \theta d\phi^2 \right] , \quad (1)$$

where the q and the conformal function Φ are functions of \bar{r} and θ . The extrinsic curvature has only $\bar{r}\phi$ and $\theta\phi$ components, and in the Brill-Brandt-Seidel notation those are denoted in terms of \widehat{H}_E and \widehat{H}_F , conformally related functions of \bar{r}, θ as

$$K_{\bar{r}\phi} = \bar{r}^{-2}\Phi^{-2}\widehat{H}_E \sin^2 \theta , \quad K_{\theta\phi} = \bar{r}^{-1}\Phi^{-2}\widehat{H}_F \sin \theta . \quad (2)$$

The initial value equations of Einstein's theory impose no constraints on q , but the momentum constraint requires that the \widehat{H} s satisfy

$$\bar{r}\partial_{\bar{r}}(\widehat{H}_E) \sin^3 \theta + \partial_{\theta}(\widehat{H}_F \sin^2 \theta) = 0 . \quad (3)$$

The fact that in this form the momentum constraint is linear, and does not depend on the spatial geometry (i.e., is independent of both q and Φ) is what ultimately will allow the fairly simple superposition to be described below.

Once q , and \widehat{H} s solving (3), are chosen, one finds the conformal function Φ by solving the Hamiltonian constraint

$$\mathcal{L}_{\text{ham}}(\Phi) = -\Phi^{-7} \left[\widehat{H}_E^2 \sin^2 \theta + \widehat{H}_F^2 \right] / (4\bar{r}^6) , \quad (4)$$

where

$$\mathcal{L}_{\text{ham}}(\Phi) \equiv \left\{ \frac{1}{\bar{r}^2} \frac{\partial}{\partial \bar{r}} \left(\bar{r}^2 \frac{\partial}{\partial \bar{r}} \Phi \right) + \frac{1}{\bar{r}^2 \sin \theta} \frac{\partial}{\partial \theta} \left(\sin \theta \frac{\partial \Phi}{\partial \theta} \right) \right\} - \frac{\Phi}{4\bar{r}^2} \left[\bar{r} \frac{\partial}{\partial \bar{r}} \left(\bar{r} \frac{\partial}{\partial \bar{r}} q \right) + \frac{\partial^2}{\partial \theta^2} q \right] . \quad (5)$$

Note that the terms in curly brackets have the form of the flat space Laplacian.

For a Kerr hole of mass M and angular momentum parameter (angular momentum per mass) a , the forms of the functions are

$$e^{-2q_K} \equiv \frac{r^2 + a^2 \cos^2 \theta}{r^2 + a^2 + \frac{2Ma^2 r \sin^2 \theta}{r^2 + a^2 \cos^2 \theta}} , \quad (6)$$

$$\widehat{H}_{EK} = \frac{aM [(r^2 - a^2)(r^2 + a^2 \cos^2 \theta) + 2r^2(r^2 + a^2)]}{[r^2 + a^2 \cos^2 \theta]^2} , \quad (7)$$

$$\widehat{H}_{FK} = \frac{-2a^3 M r (r^2 - 2Mr + a^2)^{1/2} \cos \theta \sin^2 \theta}{[r^2 + a^2 \cos^2 \theta]^2} , \quad (8)$$

$$\Phi_K^4 = \bar{r}^{-2} \left[r^2 + a^2 + \frac{2Ma^2 r \sin^2 \theta}{r^2 + a^2 \cos^2 \theta} \right] . \quad (9)$$

Here we have used the index “ K ” to denote the Kerr form, and r is a rescaling of \bar{r} given by

$$r(\bar{r}, M, a) \equiv \bar{r} \left(1 + \frac{M+a}{2\bar{r}} \right) \left(1 + \frac{M-a}{2\bar{r}} \right) . \quad (10)$$

The solution of (4) depends not only on how we choose q, \widehat{H}_E and \widehat{H}_F , but also on the boundary conditions for Φ that are specified. To recover the Kerr solution, we must not only specify that q, \widehat{H}_E and \widehat{H}_F have the forms given in (6)–(8), we must also specify boundary conditions that $\Phi \rightarrow 1$ at $\bar{r} \rightarrow \infty$, and that Φ has a singularity at $\bar{r} = 0$ of the form $\Phi \rightarrow \sqrt{M^2 - a^2}/(2\bar{r})$.

To specify more general boundary conditions for (4), it is useful to write

$$\Phi = \Phi_{\text{reg}} + \Phi_{\text{sing}} , \quad (11)$$

in which Φ_{reg} is regular in the finite \bar{r}, θ, ϕ space, and $\Phi_{\text{reg}} \rightarrow 0$ at $\bar{r} \rightarrow \infty$. The physical information specifying the nature of the solution to (4) that we are seeking is put into a specific choice for Φ_{sing} . Equation (4) then takes the form

$$\mathcal{L}_{\text{ham}}(\Phi_{\text{reg}}) = -\mathcal{L}_{\text{ham}}(\Phi_{\text{sing}}) - (\Phi_{\text{sing}} + \Phi_{\text{reg}})^{-7} \left[\widehat{H}_E^2 \sin^2 \theta + \widehat{H}_F^2 \right] / (4\bar{r}^6). \quad (12)$$

This equation can be solved iteratively for Φ_{reg} , and can be viewed as a linear partial differential equation, with a known source, at each step of the iteration. The linear difference equations arising at each iterative step were solved with an explicit solver from the LAPACK package, and as a check we also solved with a successive overrelaxation routine. A compactified radial coordinate $r_c \equiv \bar{r}/(\bar{r} + c)$, reaching a finite value at $\bar{r} \rightarrow \infty$, was used, and it was found that values on the order of $c = 1$ tended to give the best accuracy.

It is instructive to “find” the Kerr geometry with the method just outlined. We start by taking q, \widehat{H}_E and \widehat{H}_F to be the Kerr functions given in (6) —(8). Next, a choice must be made for Φ_{sing} . A choice of the form

$$\Phi_{\text{sing}} = 1 + \frac{\kappa}{2\bar{r}}, \quad (13)$$

will lead to a single throat solution. If, in addition, we specify that $\kappa = \sqrt{M^2 - a^2}$, we are choosing Φ_{sing} to have the singular behavior of Φ_K , and the solution for Φ should be the Kerr conformal factor. The solution for any other nonzero choice of κ may be considered to be a distorted Kerr hole. [If κ is taken to vanish, the right hand side of (12) diverges, and the solution for Φ turns out to give a nonstandard topology, of a type discussed in the next section.] As a test of our numerical code, we have solved (12) for Kerr inputs $q_K, \widehat{H}_{EK}, \widehat{H}_{FK}$ with the singular solution in (13) and the Kerr choice $\kappa = \sqrt{M^2 - a^2}$. Numerical solutions were computed for the case $M = 1, a = 0.9$, and were found to be in excellent agreement with the analytic form Φ_K in (9). For a grid with 200 radial and 80 angular divisions, the fractional error was of order 3×10^{-5} . It should be noted that $\Phi_K \rightarrow 1 + M/(2\bar{r})$ at large \bar{r} , whereas we have made the choice $\Phi_{\text{sing}} \rightarrow 1 + \sqrt{M^2 - a^2}/(2\bar{r})$. The difference in the asymptotic behaviors is supplied by Φ_{reg} which must fall off as $\Phi_{\text{reg}} \rightarrow (M - \sqrt{M^2 - a^2})/(2\bar{r})$. We have numerically verified, with an accuracy of 0.1%, that the coefficient of the $1/\bar{r}$ term in the computation of Φ_K , is $M/2$.

As the first step in superposing Kerr holes, we take a Kerr hole, as described above, for mass M_1 and spin parameter a_1 , and in the following way we shift the hole to a coordinate position $\bar{r} = z_1, \theta = 0$: We introduce coordinates $\bar{r}_1, \theta_1, \phi$, related to our fundamental coordinates \bar{r}, θ, ϕ , by

$$\bar{r}_1 \cos \theta_1 = \bar{r} \cos \theta - z_1, \quad \bar{r}_1 \sin \theta_1 = \bar{r} \sin \theta. \quad (14)$$

In the new coordinates the metric has the same form as in (1) so a solution of the initial value equations is given by (6) – (10), with \bar{r}, θ replaced by \bar{r}_1, θ_1 , and with the mass and angular momentum parameters taken to be M_1, a_1 . We now reexpress this shifted solution in terms of the fundamental coordinates \bar{r}, θ ; we denote the resulting solution, with a subscript 1, as $\Phi_1, q_1, \widehat{H}_{E1}, \widehat{H}_{F1}$. The first two functions transform rather simply, and are given by

$$q_1(\bar{r}, \theta) = q_K(\bar{r}_1, \theta_1; M_1, a_1), \quad \Phi_1 = \Phi_K(\bar{r}_1, \theta_1; M_1, a_1), \quad (15)$$

where q_K, Φ_K are understood to be the functional forms of coordinates and parameters given in (6) and (9). In other words, these functions are given explicitly by

$$e^{-2q_1} \equiv \frac{r_1^2 + \cos^2 \theta_1}{r_1^2 + a_1^2 + \frac{2Ma_1^2 \sin^2 \theta_1}{r_1^2 + a_1^2 \cos^2 \theta_1}}, \quad (16)$$

and

$$\Phi_1^4 = \bar{r}_1^{-2} \left[r_1^2 + a_1^2 + \frac{2M_1 a_1^2 r \sin^2 \theta_1}{r_1^2 + a_1^2 \cos^2 \theta_1} \right]. \quad (17)$$

In these expressions, the symbol r_1 is to be interpreted as

$$r_1 \equiv \bar{r}_1 \left(1 + \frac{M_1 + a_1}{2\bar{r}_1} \right) \left(1 + \frac{M_1 - a_1}{2\bar{r}_1} \right), \quad (18)$$

and \bar{r}_1, θ_1 are taken to be the functions of \bar{r}, θ given by (14).

To find the shifted extrinsic curvature we simply transform the components of the tensor K_{ij} and reinterpret the results in terms of the conformally related curvature quantities $\widehat{H}_{E1}, \widehat{H}_{F1}$. This gives us

$$\bar{r}^{-2} \Phi_1^{-2} \widehat{H}_{E1} \sin^2 \theta = \frac{\partial \bar{r}_1}{\partial \bar{r}} \bar{r}_1^{-2} \Phi_K^{-2} \widehat{H}_{EK} \sin^2 \theta_1 + \frac{\partial \theta_1}{\partial \bar{r}} \bar{r}_1^{-1} \Phi_K^{-2} \widehat{H}_{FK} \sin \theta_1 \quad (19)$$

$$\bar{r}^{-1}\Phi_1^{-2}\widehat{H}_{F1}\sin\theta = \frac{\partial\bar{r}_1}{\partial\theta}\bar{r}_1^{-2}\Phi_K^{-2}\widehat{H}_{EK}\sin^2\theta_1 + \frac{\partial\theta_1}{\partial\theta}\bar{r}_1^{-1}\Phi_K^{-2}\widehat{H}_{FK}\sin\theta_1. \quad (20)$$

When these are combined with the second relation in (15) we find

$$\widehat{H}_{E1}\sin^2\theta = \left(\frac{\bar{r}}{\bar{r}_1}\right)^2 \left[\frac{\partial\bar{r}_1}{\partial\bar{r}}\widehat{H}_{EK}\sin^2\theta_1 + \bar{r}_1\frac{\partial\theta_1}{\partial\bar{r}}\widehat{H}_{FK}\sin\theta_1 \right], \quad (21)$$

$$\widehat{H}_{F1}\sin\theta = \left(\frac{\bar{r}}{\bar{r}_1}\right) \left[\frac{1}{\bar{r}_1}\frac{\partial\bar{r}_1}{\partial\theta}\widehat{H}_{EK}\sin^2\theta_1 + \frac{\partial\theta_1}{\partial\theta}\widehat{H}_{FK}\sin\theta_1 \right]. \quad (22)$$

In these equations, the expressions \widehat{H}_{EK} and \widehat{H}_{FK} are understood to be the functional forms for the Kerr geometry. That is, they are given by (7) and (8) with \bar{r}, θ, M, a replaced by $\bar{r}_1, \theta_1, M_1, a_1$. We have used Maple to verify that the solutions in (21),(22) satisfy the momentum constraint (3).

As a check on our numerical program we have used the shifted solution of (16), (19), and (20) in (12) along with the singular solution

$$\Phi_{\text{sing}} = 1 + \frac{1}{2} \frac{\sqrt{M_1^2 - a_1^2}}{\sqrt{\bar{r}^2 - 2z_1\bar{r}\cos\theta + z_1^2}}. \quad (23)$$

Equation (12) was solved numerically for Φ_{reg} . The result for Φ_{reg} is shown in Fig. 1, and is compared with the regular part of Φ_1 , the analytic solution for a single shifted hole given in (17), for a hole with $M = 0.5, J = 0.225$, and located at $z_0 = 0.1$. Part (a) shows the numerically computed result for $\Phi_{\text{reg}}^{\text{num}}$ as a function of \bar{r} and θ ; an inset shows some detail of “fine structure” in the solution. The fractional difference between the computed and the analytic solutions is plotted in part (b). These computations used a numerical grid with 1500 radial and 800 angular grid divisions. The results, both numerical and analytic, show that Φ_{reg} is maximal near the location of the throat, and — as shown in the inset — has some fine scale structure where the symmetry axis passes through the throat. The fractional difference between the computed and the analytic Φ_{reg} was found to exhibit second order convergence and, at the finest grid spacing, was less than 0.5% even near the axis, where Φ_{reg} changes on a small length scale.

In a manner similar to that just described, we can find the functions $\Phi_2, q_2, \widehat{H}_{E2}, \widehat{H}_{F2}$, describing a hole of mass M_2 and spin parameter a_2 , shifted to z_2 . We need only replace all “1” subscripts in our first shifted solution by “2.” Since the initial value equations are not linear we cannot linearly superpose the two shifted solutions, but we *can* superpose the q, \widehat{H}_E and \widehat{H}_F functions. That is, we can take

$$q = q_1 + q_2, \quad \widehat{H}_E = \widehat{H}_{E1} + \widehat{H}_{E2}, \quad \widehat{H}_F = \widehat{H}_{F1} + \widehat{H}_{F2}. \quad (24)$$

The first of these superpositions is immediate, since q is a “free choice” that is not required to satisfy any constraint. The \widehat{H} functions must satisfy the momentum constraint (3), but that constraint is linear and independent of the 3-geometry. Since the first and the second shifted solution individually satisfy the linear, geometry-independent momentum constraint, their superposition will satisfy it.

It remains to solve for the conformal factor Φ , and this requires specifying the singularity structure. We do this by taking

$$\Phi_{\text{sing}} - 1 = (\Phi_{\text{sing1}} - 1) + (\Phi_{\text{sing2}} - 1), \quad (25)$$

where $\Phi_{\text{sing1}}, \Phi_{\text{sing2}}$ are the singular parts of Φ_1, Φ_2 . This is equivalent to taking a Newtonian-like solution

$$\Phi_{\text{sing}} = 1 + \frac{1}{2} \frac{\sqrt{M_1^2 - a_1^2}}{\sqrt{\bar{r}^2 - 2z_1\bar{r}\cos\theta + z_1^2}} + \frac{1}{2} \frac{\sqrt{M_2^2 - a_2^2}}{\sqrt{\bar{r}^2 - 2z_2\bar{r}\cos\theta + z_2^2}}. \quad (26)$$

The last step is to solve (12) numerically for Φ_{reg} .

With the numerical solution of the Hamiltonian constraint (12), we have an initial value solution for two holes, parameterized by the masses, spins, and locations of the holes. A crucial feature of this solution is that the spacetime is “locally Kerr” near the holes. Let us consider hole 1, and let us suppose that $z_1 - z_2$ is large compared to M_1 . Kerr-like coordinates can be introduced in terms of which the 3-geometry and extrinsic geometry components have approximately the form of a Kerr hole with parameters M_1, a_1 . At a radial coordinate distance r from hole 1, the fractional deviation from Kerr form will be of order $r^2/|z_1 - z_2|^2$, except for the influence of hole 2 in the conformal

factor. This correction will be of order $r/|z_1 - z_2|$. The proof of these statements is straightforward, but tedious, and the details are not given here. Instead, we present a numerical demonstration of local Kerricity for the case of identical holes ($M_1 = M_2 = 0.5, J_1 = J_2 = 0.225$) symmetrically placed about the coordinate origin ($z_1 = -z_2 \equiv z_0$).

In Fig. 2, part (a) shows $\Phi_{\text{reg}}^{\text{num}}$, the computed regular part of Φ , as a function of \bar{r} and θ . Part (b) shows $\Delta \equiv (\Phi_{\text{reg}}^{\text{num}'} - \Phi_{\text{reg}})/\Phi_{\text{reg}}$, the relative difference between the computational result and the analytic function Φ_{reg} , of (17) for a single isolated hole of $M = 0.5, J = 0.225$. Since the (two-throat) singular part for the two hole solution differs from the (one-throat) singular part for an isolated solution, the difference shown in (b) is *not* the same as the fractional difference between the $\Phi_{\text{reg}}^{\text{num}}$ and Φ_{reg} , the regular part of the shifted Kerr solution. Rather, part (b) indicates the size of $(\Phi_{\text{reg}}^{\text{num}'} - \Phi_{\text{reg}}) \equiv \Phi_{\text{reg}}^{\text{num}} - \Phi_{\text{reg}} + \sqrt{M_2^2 - a_2^2}/(2\bar{r}_2)$ with $\bar{r}_2 \equiv \sqrt{\bar{r}^2 - 2z_2\bar{r}\cos\theta + z_2^2}$. In Fig. 2 the separation parameter is $z_0 = 2.0$, and the computed hole exhibits local ‘‘Kerricity,’’ i.e., the deviation from the Kerr geometry is small, less than 4% in the neighborhood of the throat. Figure 3 shows the analogous results for a separation parameter $z_0 = 0.25$. Here, the deviation from the Kerr geometry is significantly larger, on the order of 12%. Yet smaller values of z_0 produce yet larger deviations from the Kerr geometry.

For definiteness we have described the axisymmetric superposition of two equal mass, equal spin, Kerr holes, but it should be clear that the method of superposition is more widely applicable to the axisymmetric superposition of solutions. The general principle is to put the initial value solutions to be added into the form (1). The individual metric q functions and extrinsic curvature \hat{H} functions are then superposed as in (24), and the momentum constraint (3) is guaranteed to be satisfied. The last step is to choose the singularities, and (numerically) to solve the Hamiltonian constraint for Φ_{reg} . This can be done, for an arbitrary axisymmetric array of Kerr holes, but the method is not limited to Kerr holes. Any solution that can be put in the form (1) can be superposed. In particular, the rotating holes of the Bowen-York [3] formalism can be used as building blocks. For these conformally flat solutions, $q = 0$, and superposing *only* Bowen-York holes will lead to a conformally flat initial value solution; in this case our method is simply a special case of the more general superposition that is valid in the Bowen-York formalism. More interesting is the possibility of superposing arbitrary mixtures of Bowen-York and Kerr holes, or Kerr holes with distorted Kerr holes.

III. CLOSE LIMIT SOLUTIONS

For solutions constructed by superposition as described above, the close limit is not a single Kerr hole. In the two Kerr hole solution, for example, if we let $|z_1 - z_2| \rightarrow 0$, the initial solution will have an all encompassing horizon surrounding both the throat at z_1 and at z_2 . Outside this horizon the initial value solution will *not* approach the Kerr solution. We illustrate this in Fig. 4. In part (a) we plot the computed conformal factor Φ for the superposition of two identical holes, with masses $M_1 = M_2 = 0.5$ and angular momenta $J_1 = J_2 = 0.225$, placed at $z_1 = -z_2 = z_0 = 0.02$. In part (b) we plot Δ , the relative difference between the computed solution and a Kerr solution. The comparison Kerr geometry is chosen to have angular momentum $J = J_1 + J_2 = 0.45$. For any other choice the extrinsic Kerr geometry would not agree with that for the two hole solution at large \bar{r} . By looking at the large \bar{r} behavior of the computed Φ it was determined that the two hole solution had a mass of $M = 0.824$. (This is less than $M_1 + M_2 = 1$ as should be expected.) If we were to compare our solution for Φ with a Kerr hole of any other mass, there would be unacceptable differences at large \bar{r} .

In Fig. 4, the left (small radius) boundary of the surface is at the approximate location of the initial horizon. As one would expect, the plot in (b) shows that the maximum deviation from the Kerr geometry (around 8%) occurs on the horizon. The crucial feature of these plots is that *they do not change significantly as $z_0 \rightarrow 0$* . The close limit of the two holes is not a single hole; the deviation from the Kerr geometry exhibited in part (b) does not decrease with decreasing separation. This is in clear contrast to the nonrotating case, in which the deviation outside the horizon, decreases monotonically with the separation of the holes.

There are two very different reasons for wanting a solution with a single-Kerr close limit. The first is that the evolution of a binary system will result in a single Kerr hole as the evolved close limit, so we might want an initial value solution with this feature. (This will be discussed further in the next section.) Of more practical interest, if we are to do close-limit perturbation theory, we must have a simple stationary solution as the close limit.

It is, in fact, very simple to construct a superposition with the desired close limit. We can take the metric function q and the conformally related extrinsic curvature functions \hat{H} to be precisely those of a single Kerr hole of mass and spin M, a , i.e., the functions given by (6) — (8) and (10). We could then try to impose the topology of two throats by taking Φ_{sing} to have the two-throat form of (26). But in this case, the righthand side of (12) would have a $1/\bar{r}^6$ singularity at $\bar{r} \rightarrow 0$, if $\Phi_{\text{sing}} + \Phi_{\text{reg}}$ were finite there, since \hat{H}_{EK} does not vanish at $\bar{r} \rightarrow 0$. In fact, the ‘‘nonsingular’’ function Φ_{reg} we compute diverges as $1/\sqrt{\bar{r}}$ as $\bar{r} \rightarrow 0$. With the resulting $\Phi^4 \sim \bar{r}^{-2}$ behavior of the conformal factor,

the topology of the metric is $\mathcal{R}^1 \times \mathcal{S}^2$ near $\bar{r} \rightarrow 0$. It is possible in principle for us to make Φ_{reg} truly regular by adding a term of the form $h(\theta)/\sqrt{\bar{r}}$ to Φ_{sing} . The angular function $h(\theta)$ is the solution of the nonlinear ordinary differential equation that results when the Kerr forms of $\widehat{H}_E, \widehat{H}_F$ and q , and the *ansatz* $\Phi = h(\theta)/\sqrt{\bar{r}}$ are put into (4), and the $\bar{r} \rightarrow 0$ limit is taken. Since this is numerically inconvenient, we have chosen to keep the $1/\sqrt{\bar{r}}$ singularity as a part of Φ_{reg} , and to use the boundary condition for (12) that $\sqrt{\bar{r}}\Phi_{\text{reg}}$ is regular at $\bar{r} \rightarrow 0$.

An alternative is for us to choose to add a term of the form κ/\bar{r} to Φ_{sing} . For any value of κ this will cause the extrinsic curvature term on the righthand side of (12) to vanish at $\bar{r} \rightarrow 0$. Of course, by adding such a term to Φ_{sing} , we are adding another asymptotically flat region, i.e., another throat. Our solution, then can be taken to represent an “extra” black hole. We could minimize the intrusiveness of this unwanted additional throat by choosing κ , the parameter that governs its size, to be arbitrary small. In this case, at small \bar{r} the extrinsic curvature term in (12) will become very large, of order J^2/κ^6 around $\bar{r} \sim \kappa$.

If we are to use the above choices of topology, either the $\Phi \sim 1/\sqrt{\bar{r}}$, or $\Phi \sim 1/\bar{r}$, at $\bar{r} \rightarrow 0$, we no longer have the two throat topology that represents two holes. But if this superposition is to be made only in the case the two holes are quite close, the additional central topological feature will be deep inside an all-encompassing horizon, and will be irrelevant to close-limit analysis or for numerical relativity if horizon excision is used. As we shall argue further in the next section, this means that the unwanted central topological feature in no way makes our close-limit superposition less useful. In this section we give numerical results for close-limit superpositions, and further details of how they can be used for numerical and analytic work.

In our close limit superposition to form a single Kerr hole of mass M and spin a , in addition to choosing the Kerr forms for q, \widehat{H}_E and \widehat{H}_F , we must also choose Φ_{sing} to have the form of (26), with the numerators in the second and third terms replaced by $1/2\sqrt{M^2 - a^2}$. It is only for this choice of singular structure that the mass contained in Φ_{sing} , combined with the mass coming from the solution of (12), will be the mass M in the $z_0 \rightarrow 0$ limit.

In Fig. 5 we illustrate the solution to (12) for the problem just described. For two close holes, the plots shows the relative difference between the numerically computed Φ and Φ for a single Kerr solution with the same mass and angular momentum. The initial location of the horizon is indicated. These plots demonstrate that outside the horizon Φ approaches the Kerr form as the separation between the throats (i.e., between the singularities in Φ_{sing}) is reduced. The solutions deep inside the horizon are very different, as they must be, no matter how small the separation. As explained above, for these choices there will be a formal singularity at $\bar{r}z$ corresponding to a $\mathcal{R}^1 \times \mathcal{S}^2$ feature.

So far we have presented initial data solutions in this section which can be used for close-limit analytic work, and in Sec. II we presented solutions that accurately describe two Kerr holes in the far separation limit. In the remainder of this section we will show that, with very little additional complexity, these close and far limit solutions can be combined. To simplify the description of how this is done, we will confine attention to the case of two identical holes, of parameter $M_1 = M_2 \equiv M/2$ and angular momentum $J_1 = J_2 \equiv J/2$, symmetrically placed at $z_1 = -z_2 \equiv z_0$, as in the examples of Sec. I.

To combine solutions we need to introduce a mixing function $f(z_0/M)$ that is used to weigh the amount of the far-limit solution that is to be mixed with the close limit solution. For the choice made for J_1/M_1 , let us take z_{crit} to be the largest value of z_0 for which the initial horizon encloses all throats (the two throats representing the holes, and the feature at $\bar{r} = 0$). Then the mixing function must have the property that $f = 1$ for $z_0/M > z_{\text{crit}}/M$. It must also have the close-limit property that $f \rightarrow 0$ for $z_0/M \rightarrow 0$. The mixing function might be taken, for example, to be

$$f \equiv \begin{cases} 1 & \text{for } z_0 > z_{\text{crit}} \\ 1 - (z_0 - z_{\text{crit}})^2/z_{\text{crit}}^2 & \text{for } z_0 \leq z_{\text{crit}} \end{cases} . \quad (27)$$

For our mixed solutions, we take q and the \widehat{H} functions to be

$$q = f[q_1(M_1, J_1) + q_2(M_2, J_2)] + (1 - f)q_K(M, J) , \quad (28)$$

$$\begin{aligned} \widehat{H}_E &= f[\widehat{H}_{E1}(M_1, J_1) + \widehat{H}_{E2}(M_2, J_2)] \\ &+ (1 - f)\widehat{H}_{EK}(M, J) , \end{aligned} \quad (29)$$

$$\begin{aligned} \widehat{H}_F &= f[\widehat{H}_{F1}(M_1, J_1) + \widehat{H}_{F2}(M_2, J_2)] \\ &+ (1 - f)\widehat{H}_{FK}(M, J) . \end{aligned} \quad (30)$$

For clarity we have written the expressions in (28) – (30) with parameters M_1, J_1, M_2, J_2, M, J , and have not invoked the special values of M_1, M_2, J_1, J_2 . The functions $(q_1, \widehat{H}_{E1}, \widehat{H}_{F1})$, with subscript 1, are the shifted solutions of (16), (21), and (22), and similarly for the functions with subscript 2. The functions with K subscript are the “pure” Kerr functions from (6)–(8). For the mixed solution we take the function Φ_{sing} to have the form

$$\Phi_{\text{sing}} = 1 + \frac{1}{2} \frac{f\sqrt{M_1^2 - a_1^2} + (1-f)\sqrt{M^2 - a^2}/2}{\sqrt{\bar{r}^2 - 2z_1\bar{r}\cos\theta + z_1^2}} + \frac{1}{2} \frac{f\sqrt{M_2^2 - a_2^2} + (1-f)\sqrt{M^2 - a^2}/2}{\sqrt{\bar{r}^2 - 2z_2\bar{r}\cos\theta + z_2^2}}. \quad (31)$$

For separations large enough so that a horizon does not enclose both holes, the solution, is identical to the solution of Sec. I, and therefore has the correct far limit, i.e., in the limit of large separation the solution near each throat approaches that of an isolated Kerr throat. For $z_0/M \ll 1$, the mixing function f approaches 0, and the solution approaches the Kerr solution, and hence the mixed solution must have the correct close-limit, i.e., in the limit of small separation the solution outside the horizon approaches that of a single Kerr hole.

It is interesting to note that our sequence of solutions, with mass and the angular momentum the same at large and at small separations, cannot produce a rapidly rotating final hole; for extreme individual holes, with $M_1 = J_1$, the final hole has $a = J/M^2 = 0.5$. If we want a close limit final hole that is rapidly rotating we cannot use a constant-mass, constant-angular momentum sequence. This reminds us that simply adding rotating holes does not automatically produce something of physical relevance, or at least, does not produce what we may want. This is a point we will be coming back to in the next section.

IV. SUMMARY AND CONCLUSIONS

We have presented a general method for constructing axially symmetric superpositions of Kerr black holes. The crucial feature of this method is the adoption of a 3-metric form, that of (1), with which the momentum constraint for the conformally related extrinsic curvature reduces to a linear equation, independent of the 3-geometry. In this limited sense, the approach has the simplicity of the Bowen-York [3] conformally flat approach.

In the case of sizeable separation between the superposed holes, the method produces holes with “local Kerricity,” and has the advantage of great simplicity and easy numerical implementation. The method has been illustrated with numerical results for two equivalent (equal mass, equal spin) holes, but many extensions are possible. It should be clear how to superpose any number of holes with “local Kerricity,” or holes without local Kerricity, in particular locally Bowen-York holes.

A crucial feature of our superposed solutions is that their close-limit is *not* a single Kerr hole outside the horizon. We have argued that unlike the spherically symmetric case, it should be expected on physical grounds that two locally Kerr holes, no matter how close they are, will not superpose into a single Kerr hole. Though the “failure” of the close limit is physically correct, it is inconvenient. We would like to do close limit perturbation theory, which will at the very least be of value for checking numerical codes for colliding rotating holes. We wish to emphasize that the *correct* close limit data for two holes, is the data produced by the evolution of a pair of holes falling into each other. A guess at what that initial data solution is, has little chance of being accurate. This was true, of course, also for initial data solutions representing nonrotating black holes, but in that case the variety of choices was small, and the radiation evolving from the close limit initial data seemed to be rather insensitive to the choice of details. This is very unlikely to be the case for rotating holes; here the richness of the geometry and extrinsic curvature gives a much greater scope of choices.

For the reasons just given, our focus is on close limit calculations as a check on numerical relativity calculations, so definitiveness and simple implementation are of importance. We have given, in Sec. III, an alternative superposition scheme, which is very easily implemented, and which has the correct close limit, but it has a singularity at the midpoint between two equal holes. That singularity will be hidden deep inside the horizon of a close limit solution, and is of concern only for numerical relativity methods that require a solution throughout the interior of the horizon. The presence of the singularity does not in any way suggest that the solution outside the horizon is a good or bad representation of the late stage of infall of two Kerr holes, or whether the radiation produced outside the horizon is for any reason a good or bad test of numerical relativity.

Having the singularity hidden inside the horizon means of course, that this type of initial data is only applicable in the close limit. Since it may be useful to have a sequence of solutions which includes both large and small separations, we have also given, in Sec. III, a method of mixing both types of superpositions so that for large separations one has locally Kerr holes and no spurious singularities, and in the close limit one approaches a single Kerr hole, and has a spurious singularity hidden inside the horizon.

We intend to use the close limit, and mixed-sequence, initial data solutions as a starting point for close limit computations of radiation. We have already converted the superposition solutions, in the close limit, to Cauchy data for the Teukolsky equation [24] and will be evolving a number of examples. With the technical tools in place to do studies of evolution to a rapidly rotating hole, we will be able to answer a number of interesting questions, such as the range of validity of the slow rotation limit.

ACKNOWLEDGMENTS

We thank John Baker and Raymond Puzio for helpful suggestions. This work was partially supported by NSF grant PHY-9507719.

- [1] É. É. Flanagan and S. A. Hughes, preprint gr-qc 9701039.
- [2] L. S. Finn, *A numerical approach to binary black hole coalescence*, to appear in the conference proceedings of GR14, gr-qc/9603004.
- [3] J. Bowen and J. W. York, Jr., Phys. Rev. D **21**, 2047 (1980).
- [4] A. Abrahams and R. H. Price, Phys. Rev. D **53**, 1963 (1996).
- [5] Phys. Rev. Lett. **80**, 1812 (1998).
- [6] R. H. Price and J. Pullin, Phys. Rev. Lett. **72**, 3297 (1994).
- [7] P. Anninos, R. H. Price, J. Pullin, E. Seidel and W.-M. Suen, Phys. Rev. D **52**, 4462 (1995).
- [8] R. Gleiser, O. Nicasio, R. Price, J. Pullin, Phys. Rev. Lett. **77**, 4483 (1996).
- [9] R. Gleiser, O. Nicasio, R. Price, J. Pullin (in preparation).
- [10] R. Gleiser, O. Nicasio, R. Price, J. Pullin, gr-qc/9710096, submitted to Phys. Rev. D.
- [11] R. Gleiser, O. Nicasio, R. Price, J. Pullin, Class. Quan. Grav. **13**, 117 (1996).
- [12] J. Baker, A. Abrahams, P. Anninos, S. Brandt, R. Price, J. Pullin, E. Seidel, Phys. Rev. D **55**, 829 (1997).
- [13] R. Gleiser, O. Nicasio, R. Price, J. Pullin, gr-qc/9802063, submitted to Phys. Rev.
- [14] R. Gleiser, Class. Quan. Grav. **14**, 1911 (1997).
- [15] J. Pullin, Fields Inst. Commun., **15** 117 (1997).
- [16] C. Misner, Phys. Rev. **118**, 1110 (1960).
- [17] D. Brill, R. Lindquist, Phys. Rev. **131**, 471 (1964).
- [18] A. Abrahams and R. H. Price, Phys. Rev. D **53**, 1972 (1996).
- [19] J. Baker and R. S. Puzio, preprint gr-qc/9802006.
- [20] D. Brill, Ann. Phys. (N. Y.) **7**, 466 (1959).
- [21] S. R. Brandt and E. Seidel, Phys. Rev. D **52**, 852 (1995).
- [22] S. R. Brandt and E. Seidel, Phys. Rev. D **52**, 870 (1995).
- [23] S. R. Brandt and E. Seidel, Phys. Rev. D **54**, 1403(1996).
- [24] S. A. Teukolsky, Phys. Rev. Lett. **29**, 1114 (1972).

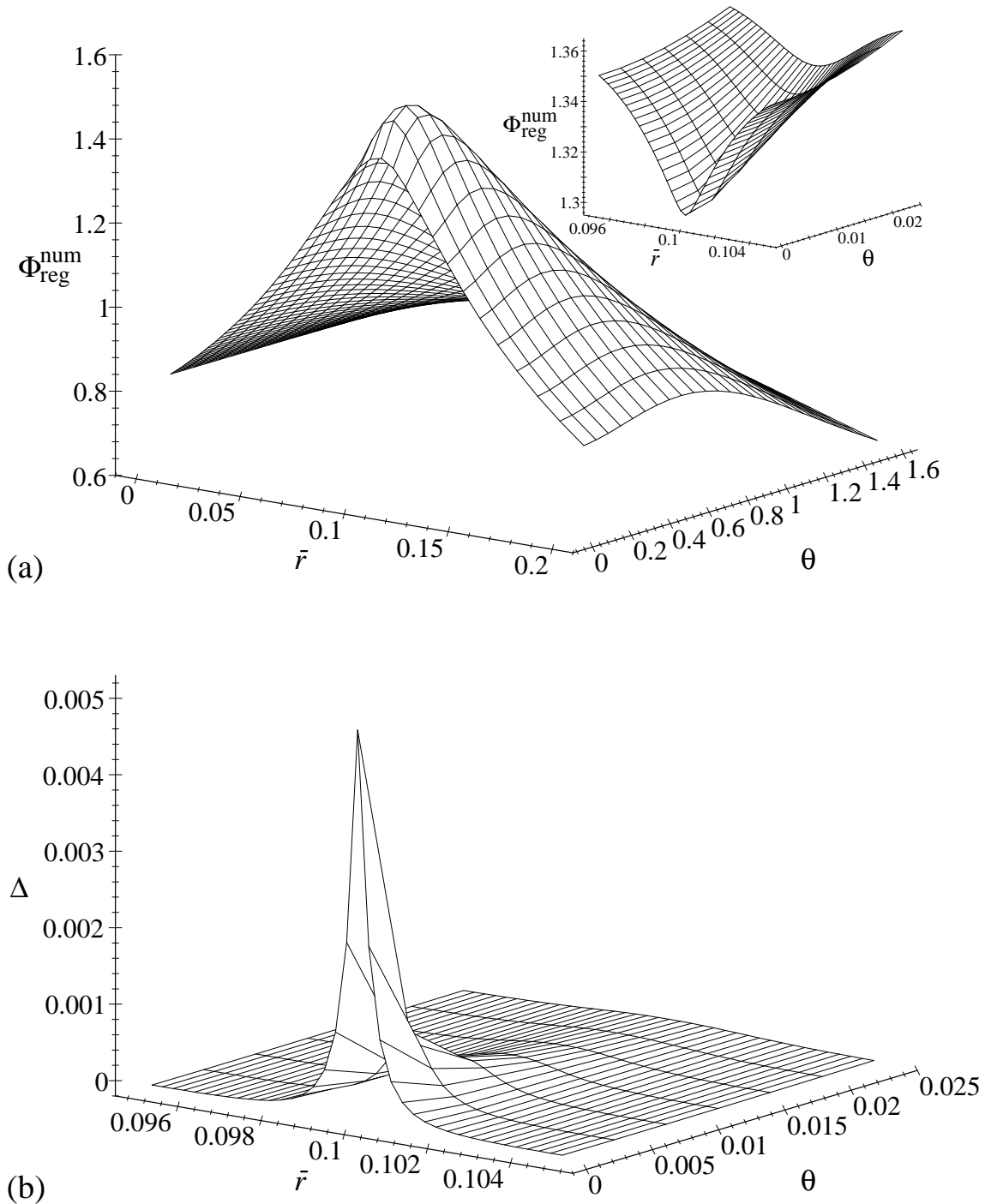
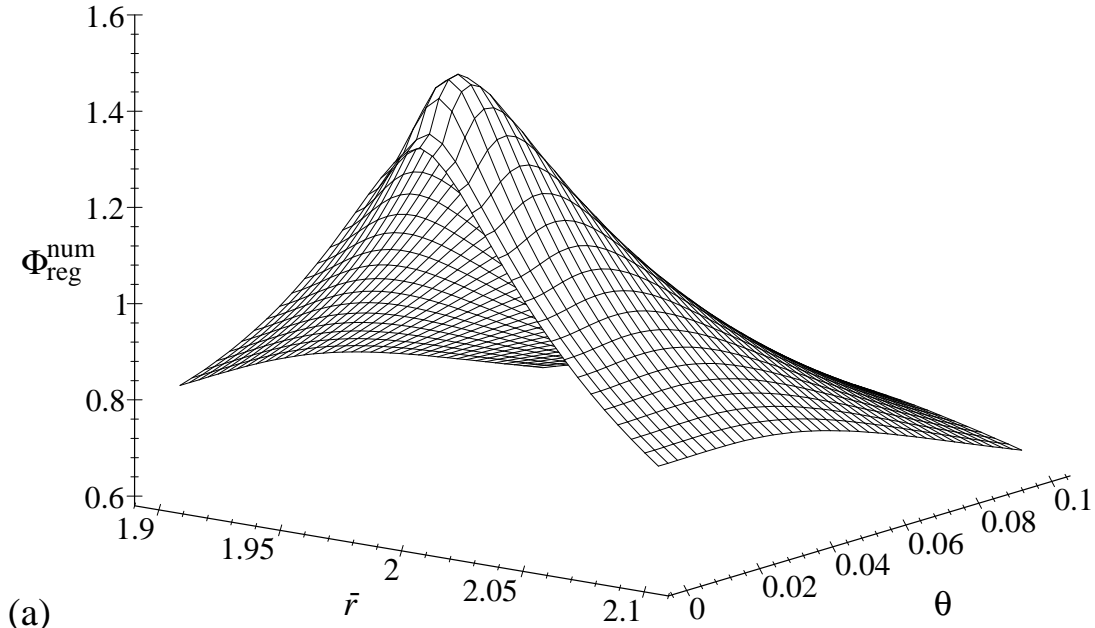
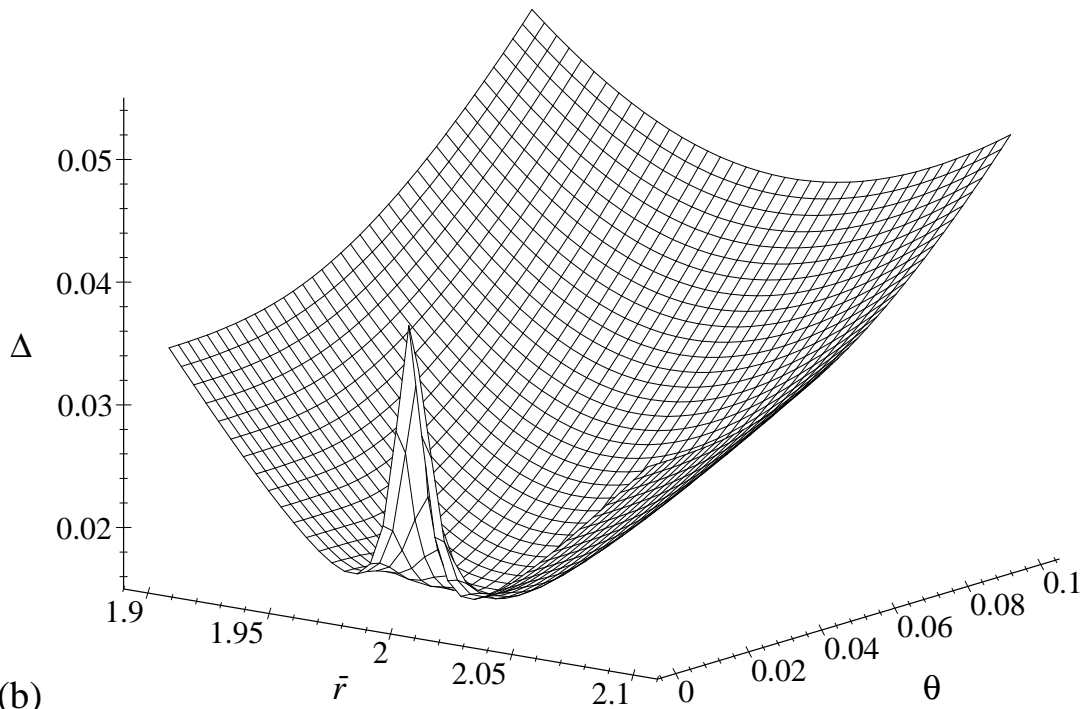


FIG. 1. (a) Numerically computed $\Phi_{\text{reg}}^{\text{num}}$ for one single Kerr black hole with $M = 0.5$, $a = 0.45$, located at $\bar{r} = z_0 = 0.1$ and $\theta = 0$. Details of the functional behavior near the singularity are displayed in the inset. (b) The relative difference, $\Delta \equiv (\Phi_{\text{reg}}^{\text{num}} - \Phi_{\text{reg}})/\Phi_{\text{reg}}$, between the numerical result $\Phi_{\text{reg}}^{\text{num}}$ and the analytic expression for the regular part Φ_{reg} , for a single shifted hole. The difference is shown in a neighborhood of the singularity.



(a)



(b)

FIG. 2. (a) $\Phi_{\text{reg}}^{\text{num}}$, computed for two black holes with masses $M_1 = M_2 = 0.5$ and angular momenta $J_1 = J_2 = 0.225$, separated by a coordinate distance $\bar{r} = 2z_0 = 4.0$. (b) The relative difference, $\Delta \equiv (\Phi_{\text{reg}}^{\text{num}} - \Phi_{\text{reg}})/\Phi_{\text{reg}}$, between the computed function $\Phi_{\text{reg}}^{\text{num}}$ and the analytic expression for Φ_{reg} for a single shifted Kerr hole of the same mass and angular momentum. See text for details.

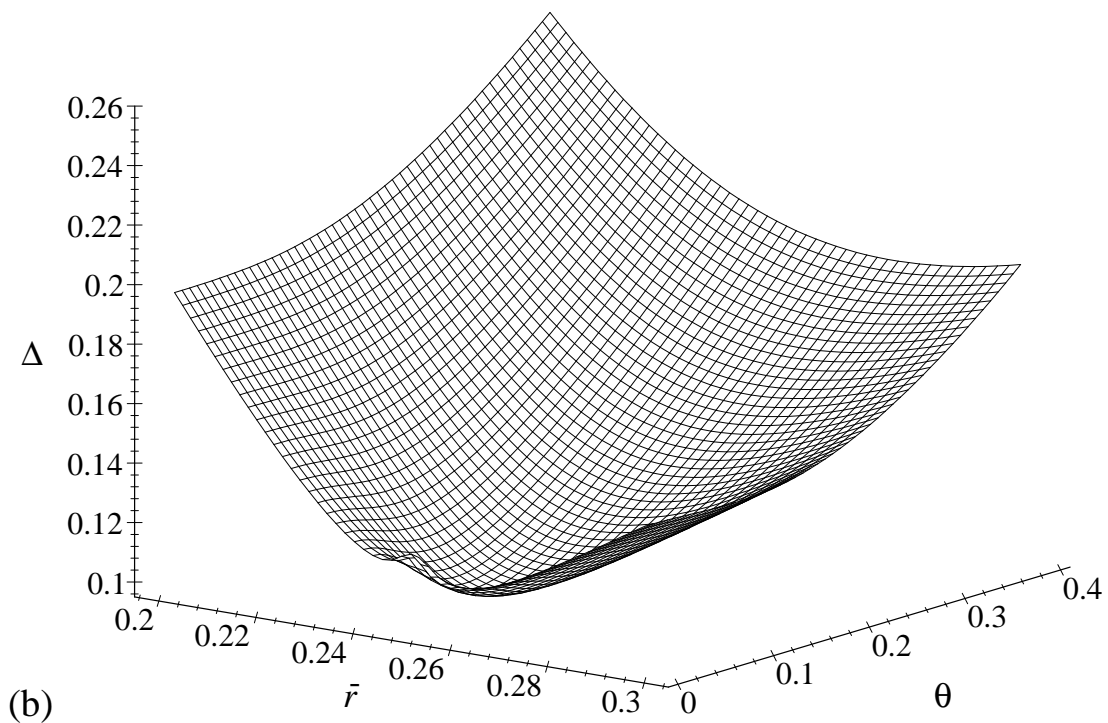
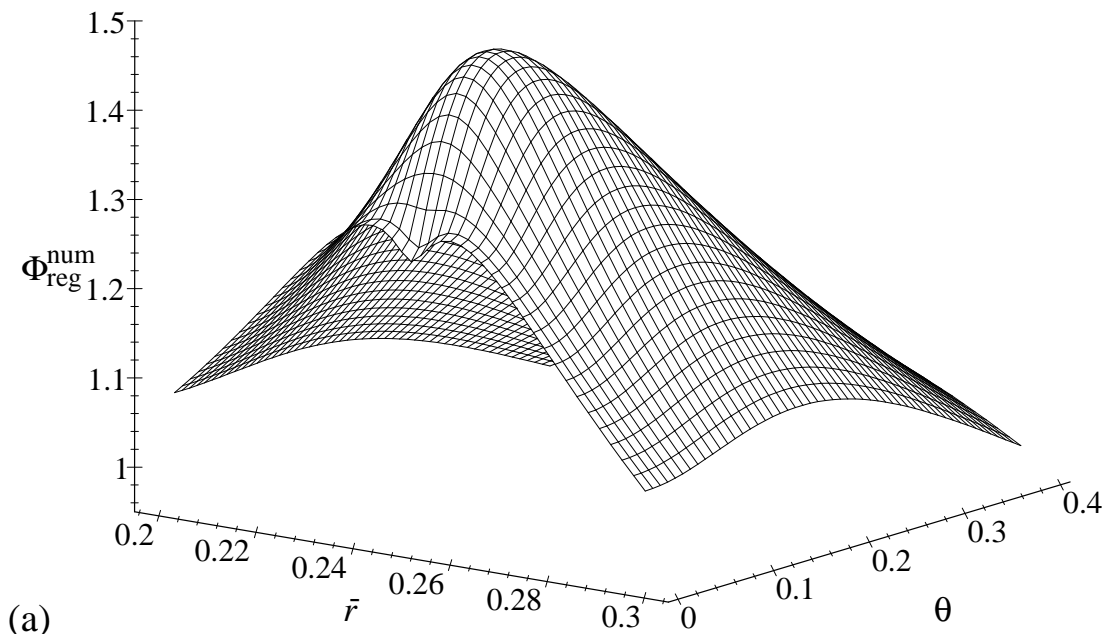


FIG. 3. Identical to Figure 2 except that $2z_0 = 0.5$. At this smaller separation of the throats, the holes lose local “Kerricity”.

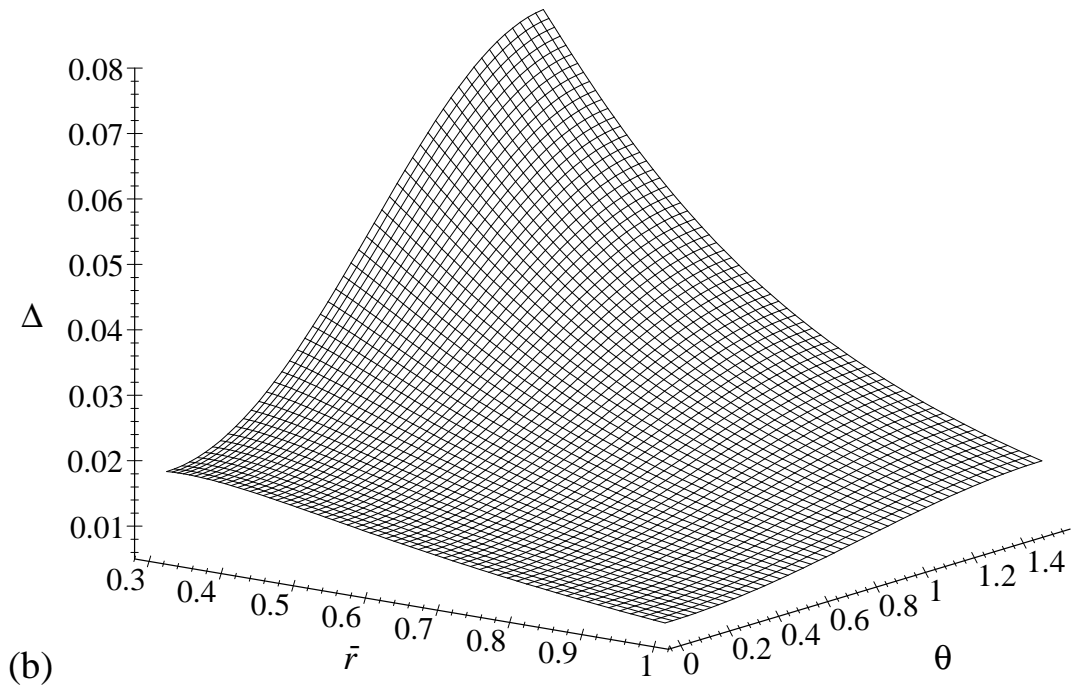
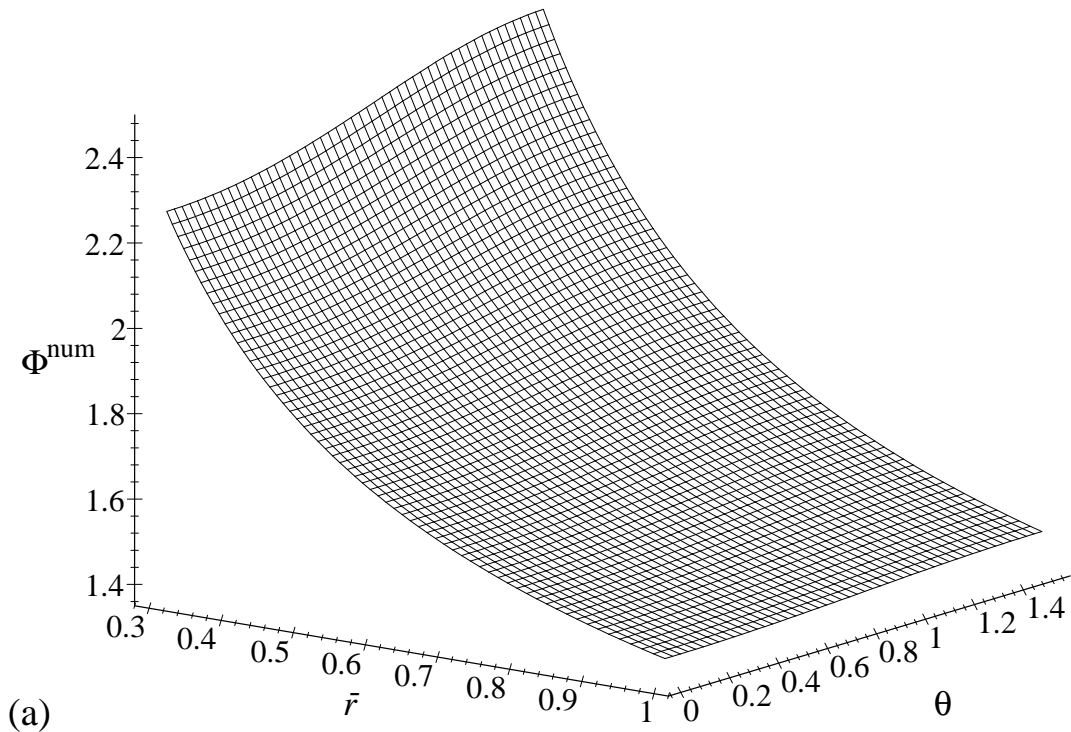


FIG. 4. The conformal factor in the close limit. Part (a) shows Φ^{num} , the conformal factor computed for two holes with equal masses $M_1 = M_2 = 0.5$ and equal angular momenta $J_1 = J_2 = 0.225$, placed symmetrically at $z_1 = 0.02$ and $z_2 = -0.02$. Part (b) shows the fractional difference $\Delta \equiv (\Phi^{\text{num}} - \Phi_K)/\Phi_K$ between the two hole solution and the conformal factor Φ_K for a Kerr hole of the same angular momentum and mass. See text for details.

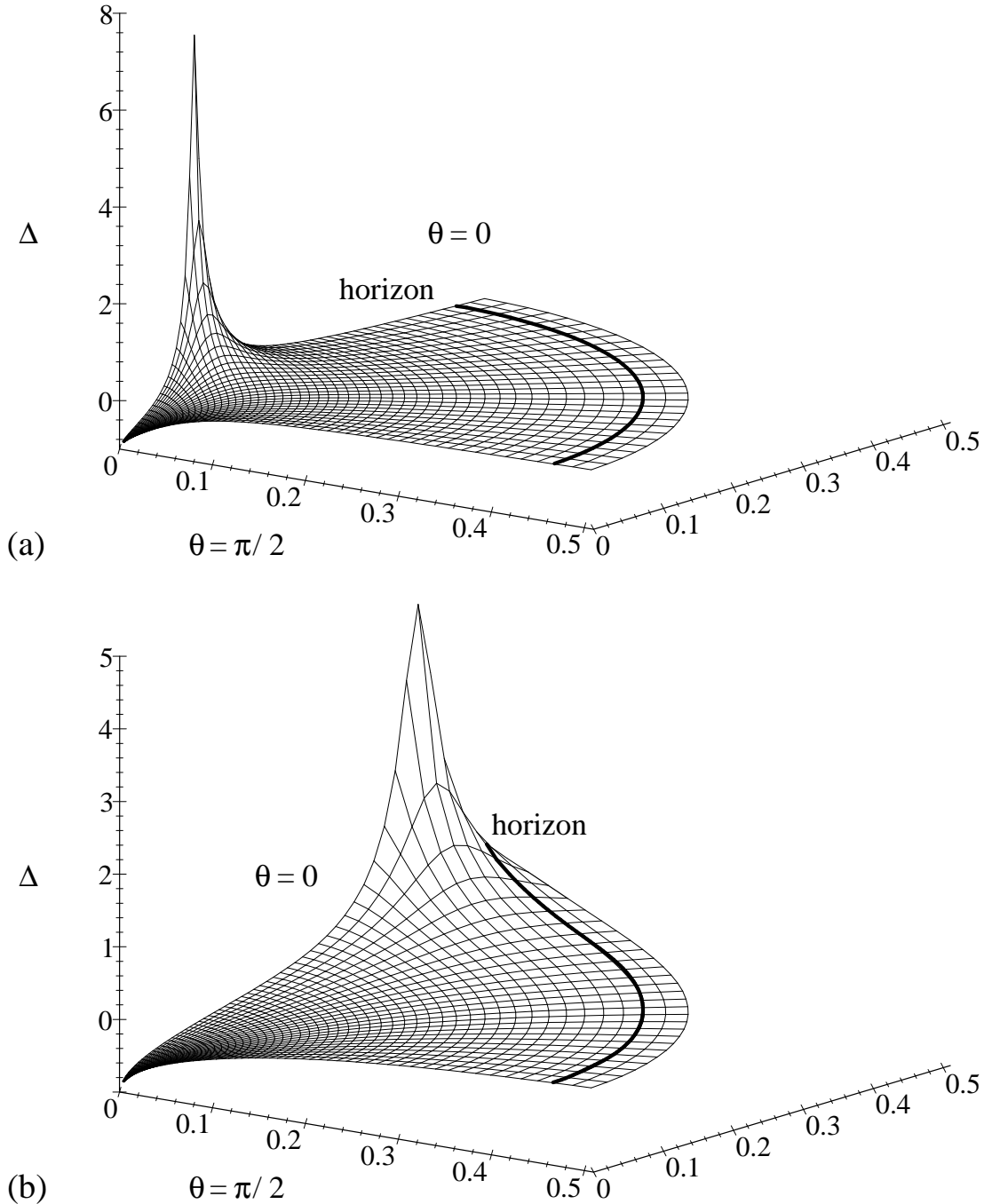


FIG. 5. The fractional difference $\Delta \equiv (\Phi^{\text{num}} - \Phi_K)/\Phi_K$ between Φ^{num} , the numerically computed conformal factor for $M = 1.0, J = 0.45$ and Φ_K , the conformal factor for a Kerr hole of the same mass and angular momentum. In (a), the separation is given by $2z_0 = 0.2$, and the difference is less than 8% outside the horizon (shown as a thick curve). In (b), $2z_0 = 0.8$, and there is a sizeable difference between the close-limit and the Kerr conformal factors.